Supplementary Figures and Tables

Burkard et al., **Accessory heterozygous mutations in cone photoreceptor *CNGA3* exacerbate CNG channel-associated retinopathy**

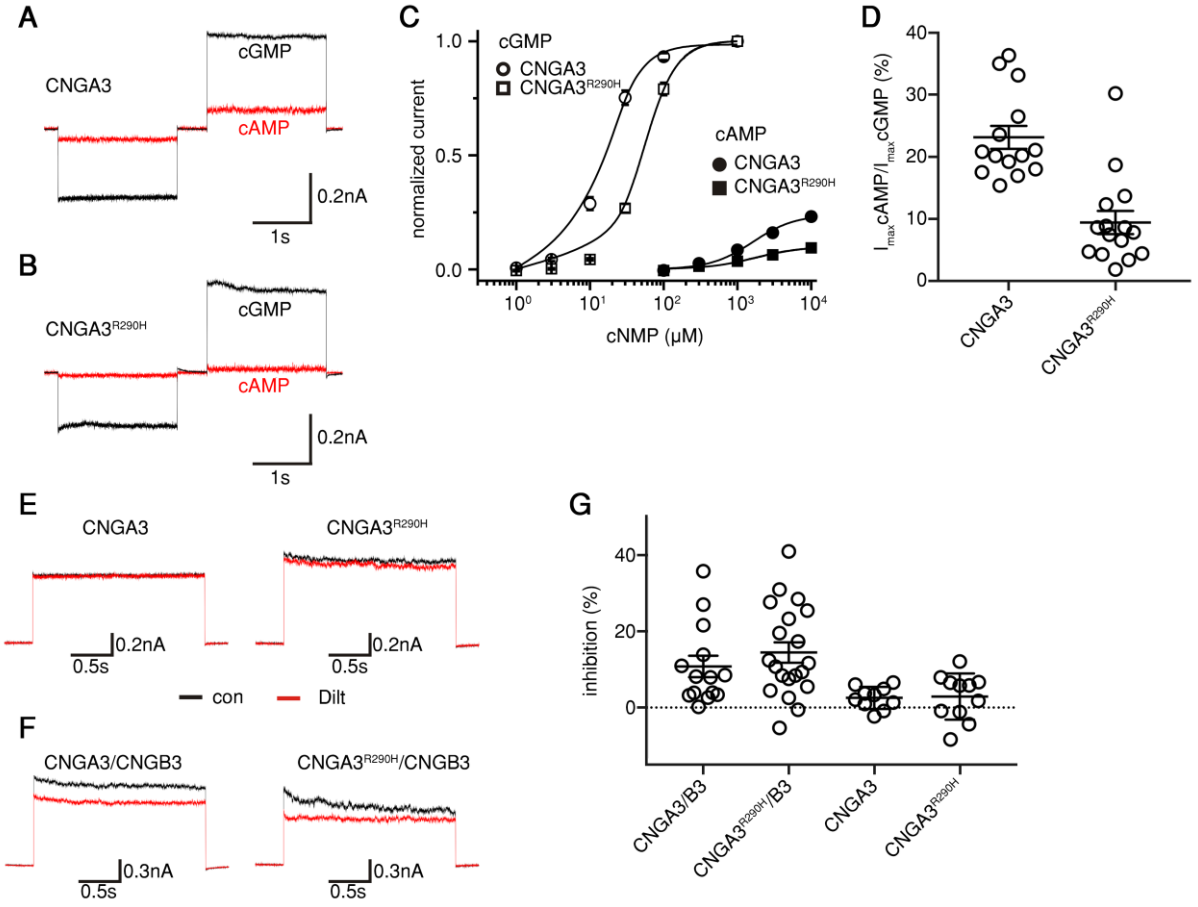

Supplementary Figure 1: hCNGA3-R290H has low affinity for cGMP. A, B: Representative current traces of wildtype hCNGA3 (A) or mutant hCNGA3-R290H channels (B) activated by 1 mM cGMP (black) and 10 mM cAMP (red) at -80 mV and +80 mV. C: Dose-response relationships for activation of wildtype hCNGA3 (circles) and mutant hCNGA3-R290H (squares) channels by cGMP (open symbols) or cAMP (filled symbols). Currents were normalized to the maximum current activated by 1 mM cGMP at +80 mV. Continuous curves represent fits of the dose-response relationship to the Hill equation. Parameters for each curve were as follows: hCNGA3wt, $k_{1/2cGMP}$=16.1 µM, ν=1.82, n=11; $k_{1/2cAMP}$=1617 µM, ν=1.52, n=14; hCNGA3-R290H, $k_{1/2cGMP}$=50.6 µM, ν=1.93, n=13; $k_{1/2cAMP}$=1707 µM, ν=1.35, n=15. Data are presented as mean ± SEM.
hCNGA3-R290H shows a low efficacy for cAMP. D: Dot plot showing the relative efficacy of cAMP for wildtype hCNGA3 (n=14) and mutant hCNGA3-R290H (n=15) channels. Currents were measured with 1 mM cGMP and 10 mM cAMP +80 mV. Data are presented as mean ± SEM. The open circles represent individual values.
hCNGA3-R290H functionally interacts with hCNGB3. E, F: Representative current traces of the homomeric (E) or heteromeric (F, + hCNGB3) wildtype hCNGA3 (left) and mutant hCNGA3-R290H channels (right) activated by 0.3 mM cGMP in the absence (black) and presence (red) of 50 µM L-cis-diltiazem at +80 mV. Sensitivity to L-cis-diltiazem (conferred by the hCNGB3 subunit) is also seen in the mutant channel, confirming assembly of heteromeric mutant hCNGA3-R290H/hCNGB3 channel complexes. G: Dot plot showing the inhibition of wildtype hCNGA3/hCNGB3 (A3/B3) (n=14) or hCNGA3 (A3) (n=10) and mutant hCNGA3-R290H/hCNGB3 ($A3^{R290H}$/B3) (n=20) or hCNGA3-R290H ($A3^{R290H}$) (n=11) channels by 50 µM L-cis-diltiazem. Data are presented as mean ± SEM. The open circles represent individual values.

A

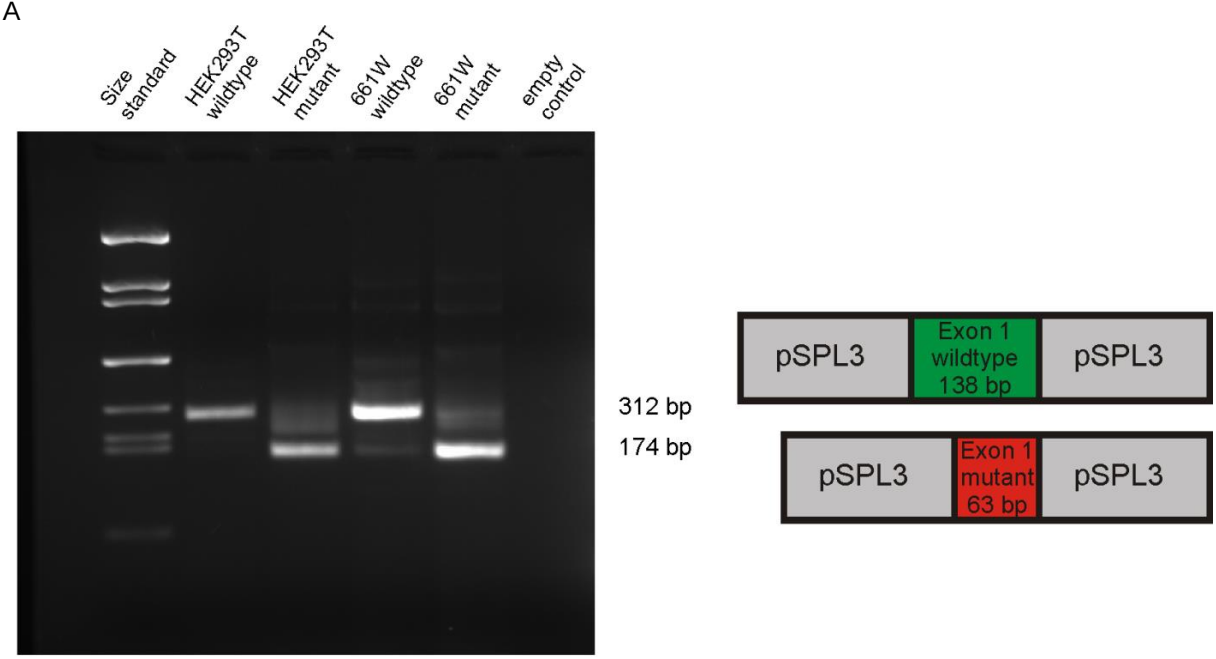

B

Wildtype Exon 1 cDNA Sequence resulting from c.-37-1G

```
pSPL3-CAATCATCTG GGGGGCTAAA TGTGACAAAC CGAGAAGATG GCCAAGATCA ACACCCAATA CTCCCACCCC
                                              -M- -A--K--I-- N--T--Q--Y --S--H--P-

novel splice acceptor
 TCCAGGACCC ACCTCAAGGT AAAGACCTCA GACCGAGATC TCAATCGCGC TGAAAATGGC CTCAGCAG-pSPL3
 -S--R--T-- H--L--K--V --K--T--S-- D--R--D-- L--N--R--A--E--N--G- -L--S--R
pSPL3-GACCC ACCTCAAGGT AAAGACCTCA GACCGAGATC TCAATCGCGC TGAAAATGGC CTCAGCAG-pSPL3
```

Mutant Exon 1 cDNA Sequence resulting from c.-37-1C

Supplementary Figure 2: In vitro splicing assay for *CNGA3* c.-37-1G>C. A: RT-PCR revealed an aberrant, smaller (174 bp) transcript in both HEK293T and 661W cells transfected with the mutant compared to the wildtype construct, but also small amounts of potentially correctly spliced constructs are seen (left). Schemes of the amplified cDNA products are presented on the right of the agarose gel (right). B: Sequence analysis provided evidence that the aberrant smaller transcript results from an activation of a novel splice acceptor (underlined and coded yellow), leading to the loss of 75 base pairs of the 5'UTR of exon 1, including the start codon ATG. Wildtype sequence is given in green, aberrantly spliced sequence due to the mutation c.-37-1G>C is given in red. pSPL3-vector exons are marked with grey boxes. Protein sequence for the wildtype is given below DNA sequence in the one letter amino acid code.

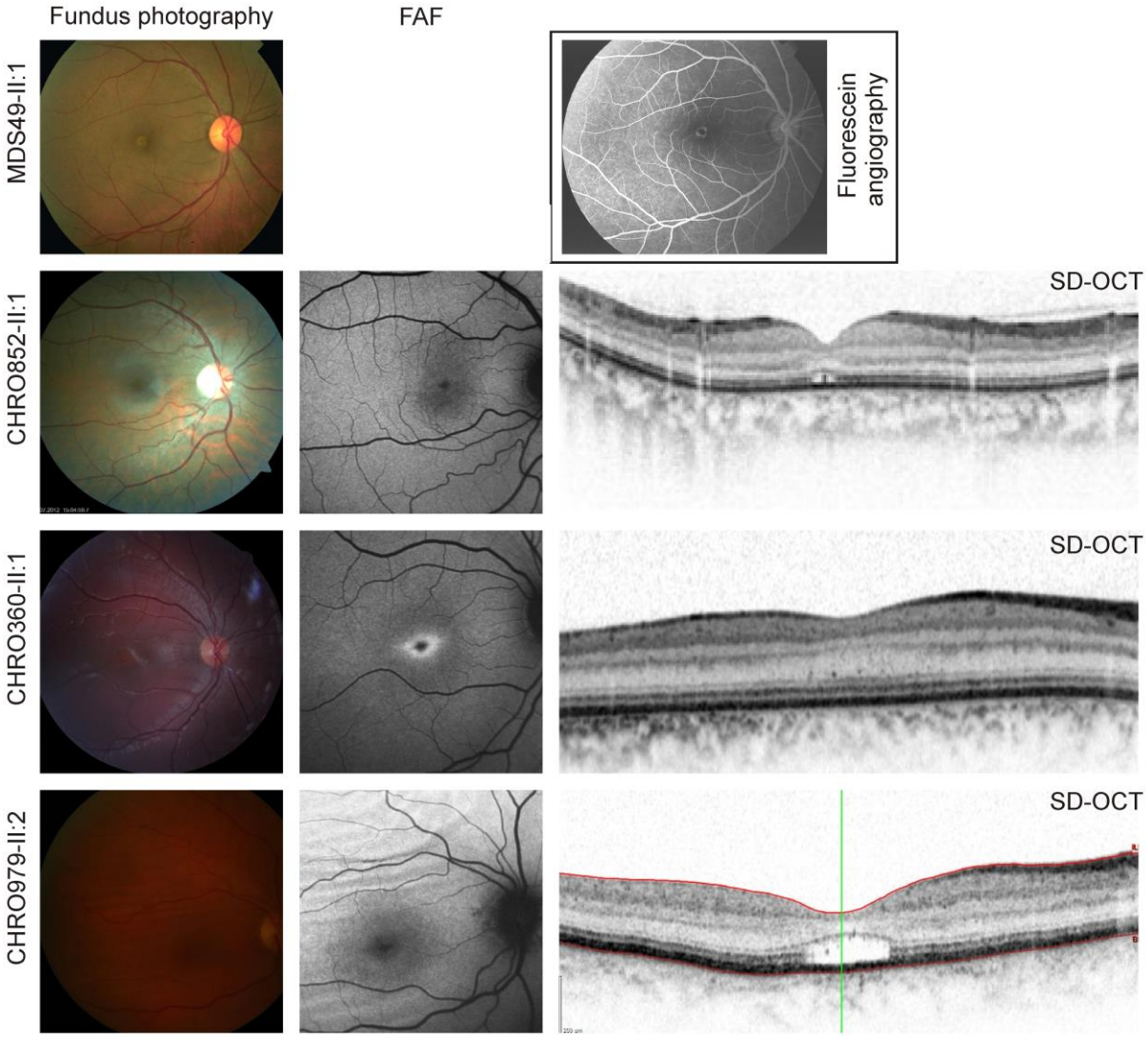

Supplementary Figure 3: Exemplary morphological fundus presentation documented photographically by fundus autofluorescence photography (FAF) and spectral-domain optical coherence tomography (SD-OCT) of representative patients from the four different genotype and disease severity groups.

The right eye is shown. From top to bottom: For patient MDS49-II:1 (age 48 y) no SD-OCT and FAF image was available, fluorescein angiography for this patient is shown instead (1). This patient is homozygous for the missense mutation c.1208G>A;p.R403Q in *CNGB3*. The initial clinical diagnosis of adult vitelliform macular dystrophy was based on a small, circular yellowish lesion in the fovea, with corresponding delicate hyperfluorescence in the angiographic image. CHRO360-II:1 (age 11 y) is compound heterozygous for *CNGB3*/c.1148delC;p.T383Ifs*13 and c.1208G>A;p.R403Q, and presented with normal retinal appearance in fundus photography. In FAF a target-shaped hyperfluorescence was found. SD-OCT findings showed foveal hypoplasia with a continuous inner segment ellipsoid layer (ISe). CHRO852-II:1 (age 22 y) with a clinical diagnosis of incomplete ACHM carries the homozygous mutation c.1208G>A;p.R403Q in *CNGB3* and an additional heterozygous missense mutation c.869G>A;p.R290H in *CNGA3*. Funduscopy showed mild foveal pigment mottling. SD-OCT imaging revealed a small inner segment ellipsoid (ISe) layer disruption. CHRO979-II:2 (age 53 y) is compound heterozygous for a splice defect c.1578+1G>A and c.1208G>A;p.R403Q in *CNGB3* and an additional heterozygous nonsense mutation c.1320G>A p.W440* in *CNGA3*. This patient shows a more severe phenotype with a larger disruption of the ISe band and a foveolar empty cavity, but the patient is also the oldest patient presented. The patient also had choroidal folds associated with high hyperopia.

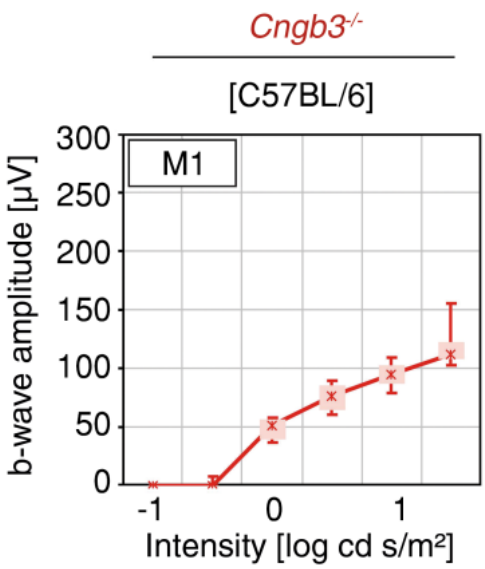

Supplementary Figure 4: Severely depressed ERG b-wave in photopic flash analysis of young *Cngb3*$^{-/-}$ mice

The b-wave amplitudes of young *Cngb3*$^{-/-}$ mice at 1 month of age (M1, C57BL6/J; n=4) were measured with photopic flash ERG protocol. Noteworthy, heterozygous *Cngb3*$^{+/-}$ mice have not been found to exhibit b-wave abnormalities (2). ERG data is depicted as box whisker plots (boxes: 25%-75% quantile range, whiskers: 5% and 95% quantiles, asterisks: median).

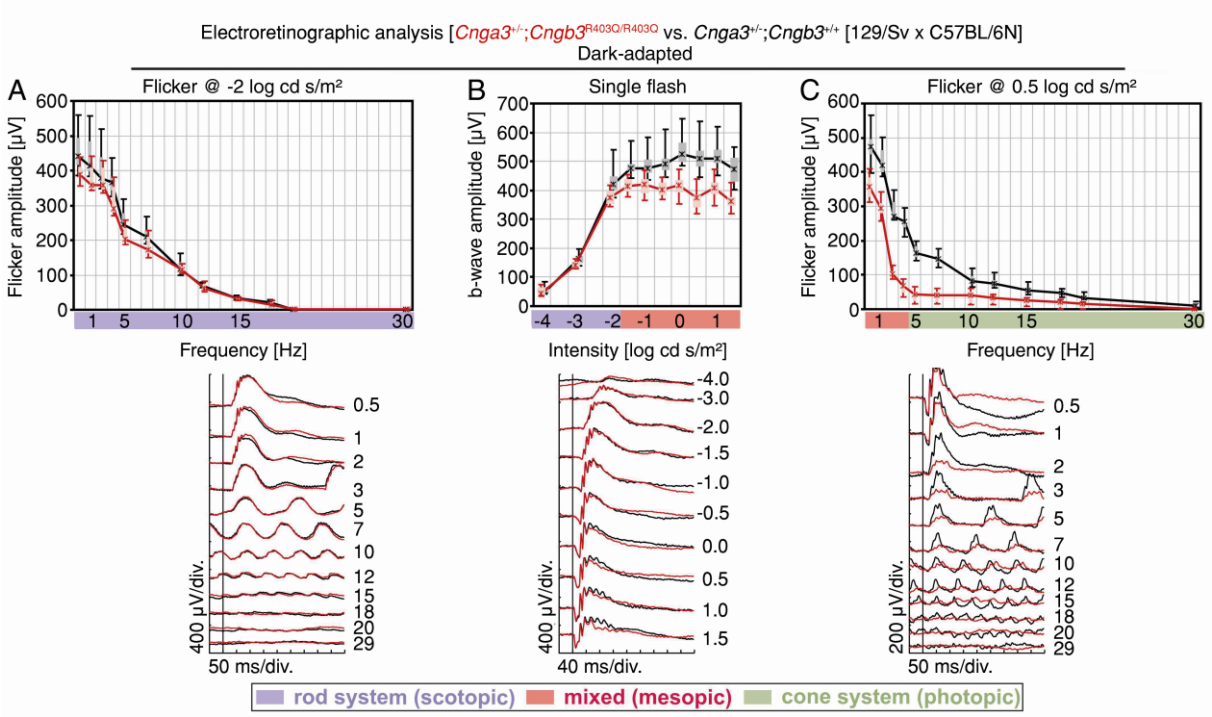

Supplementary Figure 5: Dark-adapted ERG from aged *Cnga3*$^{+/-}$;*Cngb3*$^{R403Q/R403Q}$ mice reveals stronger impairment of cone function than in *Cnga3*$^{+/-}$ controls

ERG from *Cnga3*$^{+/-}$;*Cngb3*$^{R403Q/R403Q}$ (red) compared to *Cnga3*$^{+/-}$ controls (black) on 129/Sv x C57BL/6N background. Mice (n=3) were tested at 7-12 months of age. A: Dark flicker ERG. B: Scotopic single flash ERG. C: Scotopic flicker ERG. ERG data is depicted as box whisker plots (boxes: 25%-75% quantile range, whiskers: 5% and 95% quantiles, asterisks: median).

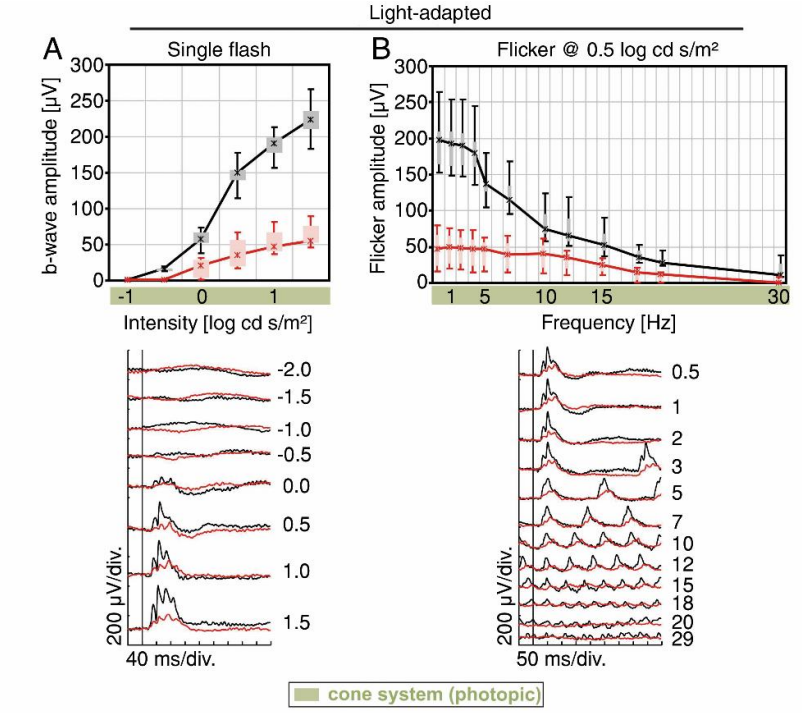

Supplementary Figure 6: Light-adapted ERG from aged *Cnga3*$^{+/-}$;*Cngb3*$^{R403Q/R403Q}$ mice reveals stronger impairment of cone function than in *Cnga3*$^{+/-}$ controls

ERG from *Cnga3*$^{+/-}$;*Cngb3*$^{R403Q/R403Q}$ mice (red) compared to *Cnga3*$^{+/-}$ controls (black) on 129/Sv x C57BL/6N background. Mice (n=3) were tested at 7-12 months of age. A: Photopic single flash ERG. B: Photopic flicker ERG. ERG data is depicted as box whisker plots (boxes: 25%-75% quantile range, whiskers: 5% and 95% quantiles, asterisks: median).

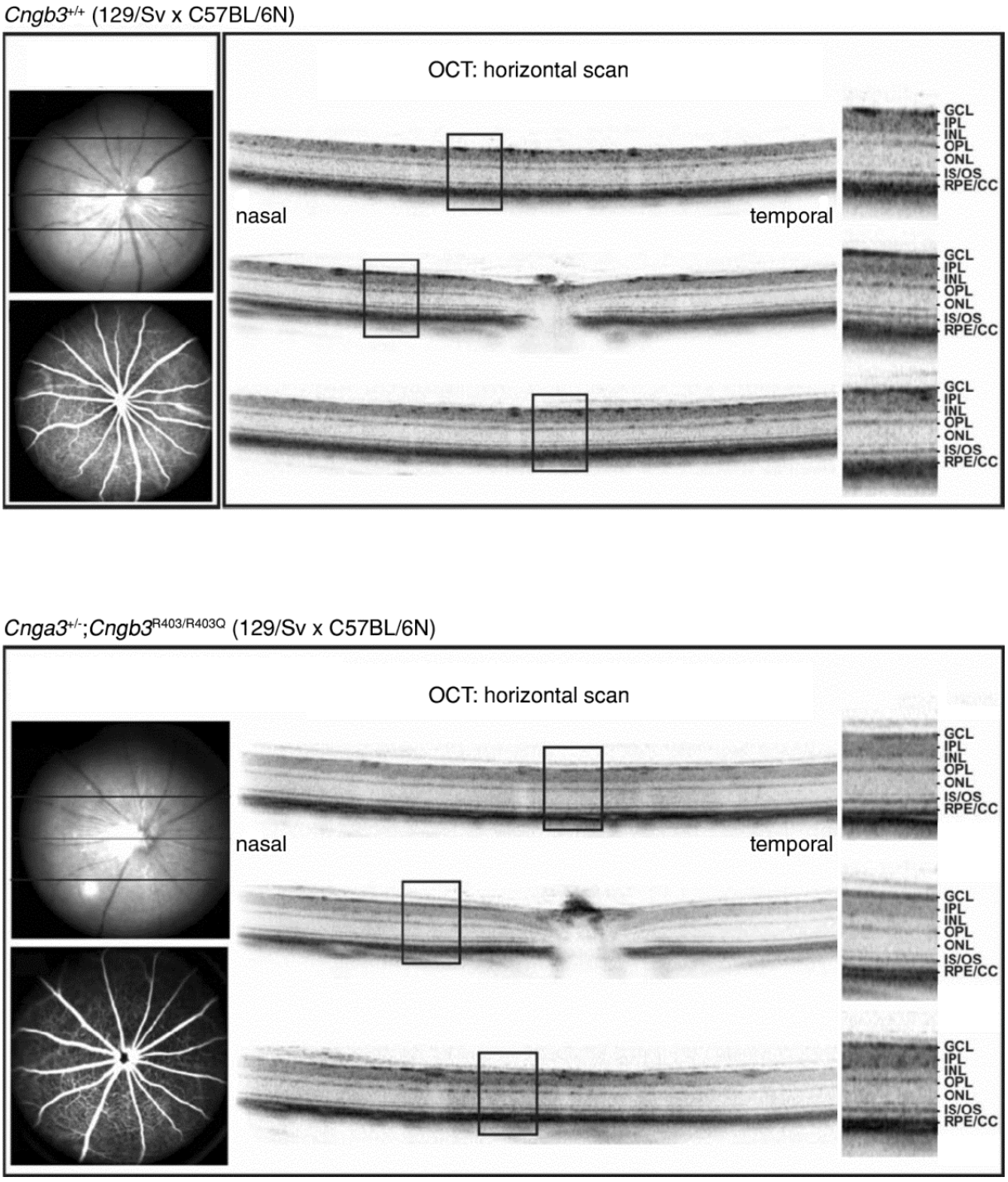

Supplementary Figure 7: Exemplary SLO and OCT scans reveal no gross abnormalities between aged *Cngb3*$^{+/+}$ wildtype and *Cnga3*$^{+/-}$;*Cngb3*$^{R403Q/R403Q}$ mutant mice.
Cngb3$^{+/+}$ (top) and *Cnga3*$^{+/-}$;*Cngb3*$^{R403Q/R403Q}$ mice (bottom) at 7-12 months of age (129/Sv x C57BL/6N; n=3) were measured with SLO (left) and OCT (right) following ERG recordings to exclude pronounced retinal degeneration in mutant mice. GCL: ganglion cell layer; INL: inner nuclear layer; IPL: inner plexiform layer; IS: inner segment; ONL: outer nuclear layer; OPL: outer plexiform layer; OS: outer segment; RPE: retinal pigment epithelium.

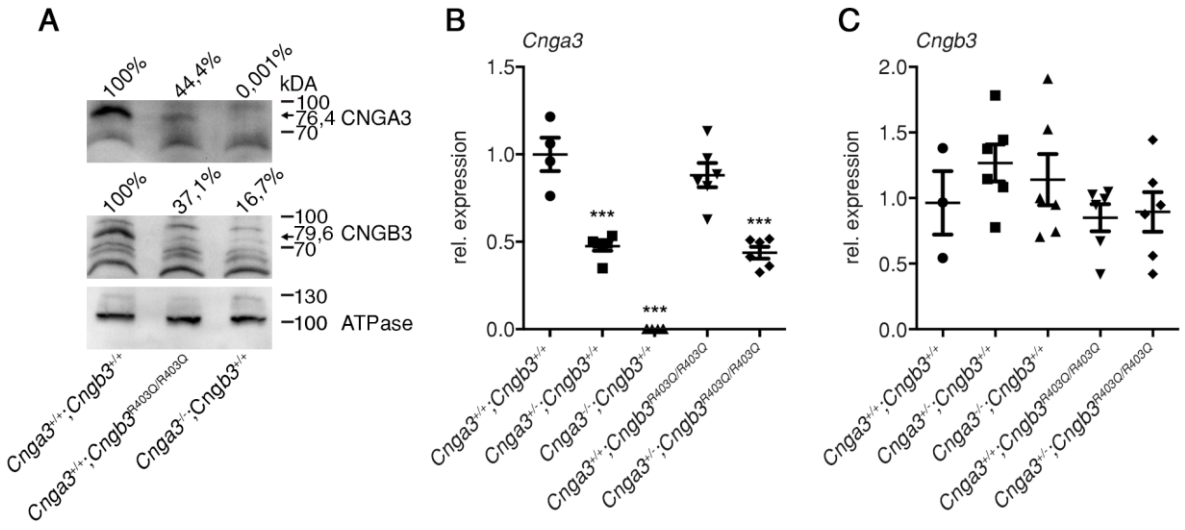

Supplementary Figure 8: Retinal protein amounts of CNG channel subunits but not transcript levels are reduced in mice homozygous for CNGB3/p.R403Q.
A: Western blot analysis of *Cngb3*$^{R403Q/R403Q}$ *retinae* (n=10) compared to wildtype (n=10) and *Cnga3*$^{-/-}$ *retinae* (n=10) with antibodies against CNGA3 (top), CNGB3 (middle) and ATPase (bottom, as loading control). B: and C: Relative transcript levels for *Cnga3* (B) and *Cngb3* (C) as determined by qRT-PCR analysis with retinal RNA from wildtype, *Cnga3*$^{+/-}$, and *Cnga3*$^{-/-}$, and mutant *Cngb3*$^{R403Q/R403Q}$, and *Cnga3*$^{+/-}$;*Cngb3*$^{R403Q/R403Q}$ 129/Sv mice at one month of age. Protein and transcript levels are normalized to wildtype mice levels. qRT-PCR data are presented as mean ± SEM (n=6 for the mutant genotypes; n=4 for *Cnga3* and n=3 for *Cngb3* wildtype controls).

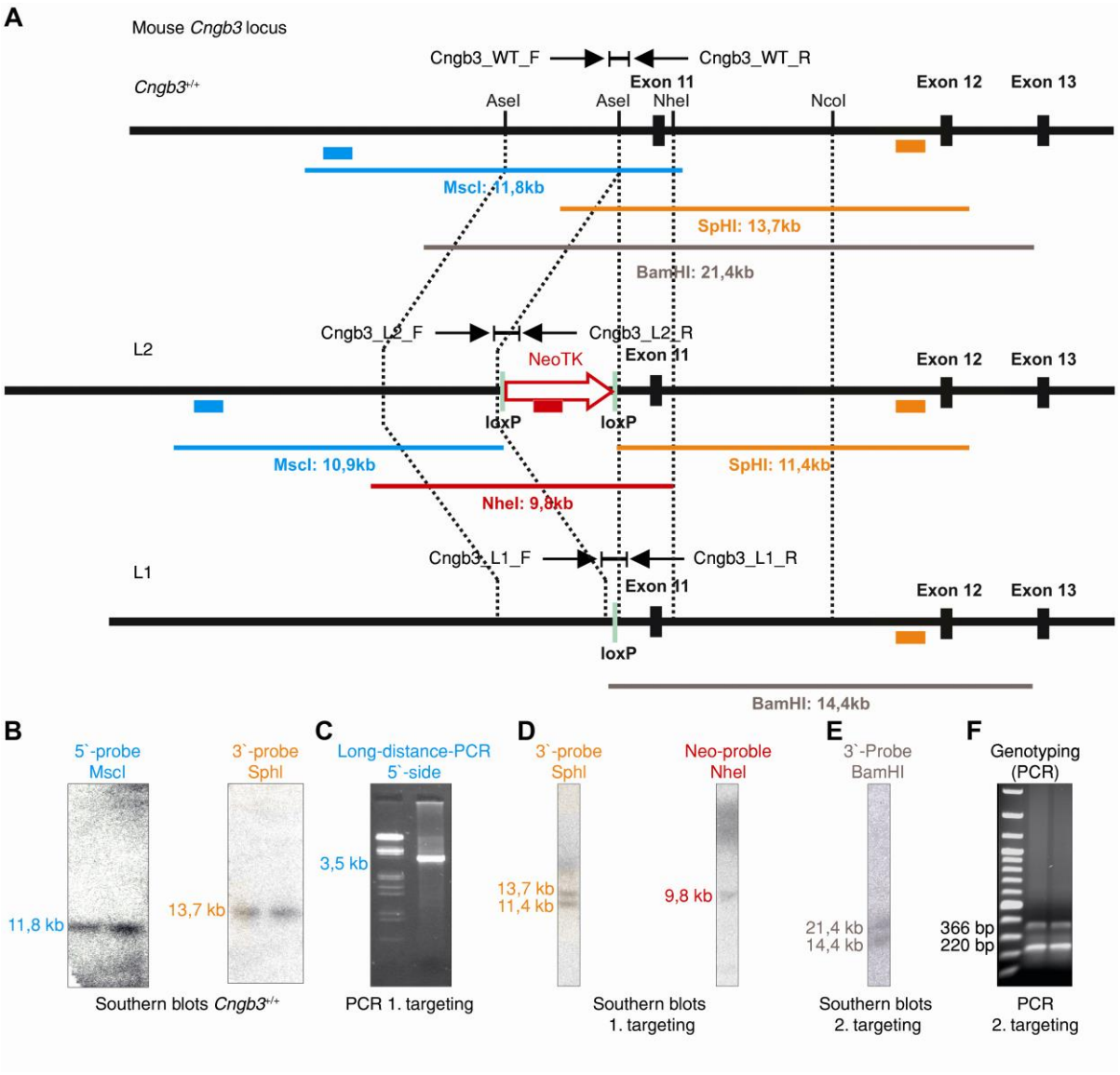

Supplementary Figure 9: Generation of the CNGB3/p.R403Q knockin mouse

A: In a first targeting experiment the targeting vector (containing the mutated exon 11^{R403Q} next to a floxed *Neo*/*TK* selection cassette and 5' [A*se*I – A*se*I fragment] and 3' homology arms [N*he*I – N*co*I fragment] was integrated into the genome of mouse embryonic stem cells by homologous recombination yielding G418-resistent ES cell clones with two loxP sites (L2). In a second targeting experiment the *Neo*/*TK* selection cassette was removed through transient expression of cre-recombinase resulting in ES cell clones containing only one loxP site (L1) next to exon 11^{R403Q}. Analysis of correct recombinant stem cell colonies was performed by Southern blot analysis (B, D, E: 5', 3', and *Neo* blot to ensure correct recombination and to exclude multiple integration of the targeting construct) and PCR analysis (C, F) after each targeting experiment. LoxP sites are indicated as short green vertical bars, PCR primer as black arrows, and Southern blot probes as horizontal bars.

Supplementary Table 1: Clinical presentation and genotype of CNGB3/p.R403Q achromatopsia. A comprehensive overview of the cases identified in this study (bold letters) and cases reported in the literature is given.

SEE SEPARATE EXCEL FILE (Supplementary Table 1)

Supplementary Table 2: Mutations and variant classification. All *CNGB3* (top) and *CNGA3* (bottom) mutations identified in the patients of this study are classified by means of prediction tools for missense, nonsense and indel variants (i.e. Mutationtaster (3), PolyPhen (4), SIFT (5) as well as potential effect on splicing (i.e. HSF, MaxEnt (6)), evolutionary conservation, recurrency in mutation databases and our in-house ACHM database, frequency in normal population (i.e. gnomAD browser), supporting functional data evidence, and finally ACMG classification (7). Variant designation is based on NCBI reference sequence for *CNGB3* (NC_000008.11, NM_019098.4;GRCh38) comprising 18 coding exons and for *CNGA3* (NC_000002.12, NM_001298.2;GRCh38) comprising 7 coding exons. Variants were submitted to ClinVar (8) under the submission no. SUB3087060. Abbreviations: MAF – minor allele frequency, PTC – premature termination codon, fs – frame-shift, TM – Transmembrane domain, CNBD – cGMP binding domain.

CNGB3 **Variant**	**Polypeptide**	**Literature /** **ClinVar annotation**	**Prediction tools** 1 Mutationtaster 2 Polyphen (Score) 3 SIFT (Score) 4 Splice site variants: HSF&MaxEnt	**Conservation** complete = CNG3/CNG1 high = CNG3 **Location in functional domain**	Variant recurrently seen in **ACHM patient cohort**	**Frequency in normal population** (gnomAD) Het/Alleles/Hom MAF in %	**Supporting functional data**	**ACMG classification**
c.112C>T	p.Q38*	Kohl et al. 2005 (9) SCV000700209	1 Disease-causing, PTC 4 HSF&MaxEnt: Potential alteration of splicing.	-	Yes	No entry	-	Pathogenic
c.819_826del	p.R274Vfs*13	Kohl et al. 2000 (10) SCV000700210	1 Disease-causing, fs, PTC 4 HSF&MaxEnt: Potential alteration of splicing.	-	Yes	17/277110/0 MAF 6.135e-3	-	Pathogenic
c.1148delC	p.T383Ifs*13	Kohl et al. 2000 (10) SCV000700211	1 Disease-causing, fs, PTC 4 HSF&MaxEnt: Potential alteration of splicing.	-	Yes	487/276004/0 MAF 0.1764	Peng et al. 2003 (11): Functional assessment by heterologous *in vitro* expression	Pathogenic
c.1208G>A	p.R403Q	Michaelides et al. 2004 (12) SCV000700212	1 Disease-causing 2 Probably damaging 0.975 3 Tolerated 0.16 4 HSF&MaxEnt: No impact on splicing.	High Pore domain	Yes	1183/276004/26 MAF 0.4274	Mouse model, this study Bright et al. 2005 (13)	Pathogenic
c.1578+1G>A		Kohl et al. 2000 (10) SCV000700213	4 HSF&MaxEnt: Alteration of the wildtype donor site, most probably affecting splicing		Yes	4/244910/0/26 MAF 1.633e-3	-	Pathogenic
c.1673G>T	p.G558V	This study SCV000700214	1 Disease-causing 2 Probably damaging 1.000 3 Damaging 0 4 HSF&MaxEnt: Potential alteration of splicing.	High Loop ß2-ß3	No, single patient; complex genotype in *cis* c.[1208G>A;1673 G>T]	No entry	-	Variant of uncertain significance
c.1783C>T	p.L595F	Nishiguchi et al. 2005 (14) SCV000700215	1 Disease-causing 2 Probably damaging 1.000 3 Damaging 0.01 4 HSF&MaxEnt: Potential alteration of splicing.	Complete Loop □6-□7	No, single patient	No entry	Meighan et al. 2015 (15)	Variant of uncertain significance

***CNGA3* Variant**	**Polypeptide**	**Literature / ClinVar annotation**	**Prediction tools** 1 Mutationtaster 2Polyphen (Score) 3 SIFT (Score) 4 Splice site variants: HSF&MaxEnt	**Conservation** complete = CNG3/CNG1 high = CNG3 **Location in functional domain**	Variant recurrently seen in **ACHM patient cohort**	**Frequency in normal population** (gnomAD) Het/Alleles/Hom MAF in %	**Supporting functional data**	**ACMG classification**
c.-37-1G>C		This study SCV000700216	No prediction possible	-	No, single patient	No entry	This study Minigene assay confirming missplicing	Likely pathogenic
c.667C>T	p.R223W	Wissinger et al. 2001 (16) SCV000700217	1 Disease-causing 2 Probably damaing 1.00 3 Damaging 0 4 HSF&MaxEnt: Potential alteration of splicing.	Complete Loop TM2-TM3	Yes	21/276872/0 MAF 7.585e-3	Muraki-Oda et al. 2007 (17)	Pathogenic
c.682G>A	p.E228K	Reuter et al. 2008; Thiadens et al. 2010 (18, 19) SCV000700218	1 Disease-causing 2 Probably damaging 0.957 3 Tolerated 0.09 4 HSF&MaxEnt: No impact on splicing.	Complete Loop TM3-TM4	Yes, 1 compound-heterozygous, 1 homozygous	354/277050/2 MAF 0.1278	Reuter et al. 2008 (18)	Pathogenic
c.796G>A	p.V266M	Thiadens et al. 2010 (19) SCV000700219	1 Polymorphism 2 Benign 0.089 3 Tolerated 0.14 4 HSF&MaxEnt: Potential alteration of splicing.	**Low** Loop TM3-TM4	No	59/246252/0/ MAF 0.02396	-	Variant of uncertain significance
c.829C>T	p.R277C	Wissinger et al. 2001 (16) SCV000700220	1 Disease-causing 2 Probably damaging 1.000 3 Damaging 0 4 HSF&MaxEnt: Potential alteration of splicing.	Complete TM4	Yes	26/246176/0 MAF 0.01056	Liu et al. 2005, Muraki-Oda et al. 2007 (17, 20),	Pathogenic
c.869G>A	p.R290H	This study SCV000700221	1 Disease-causing 2 Probably damaging 0.993 3 Tolerated 0.07 4 HSF&MaxEnt: Potential alteration of splicing.	Complete TM4	No, single patient	41/277186/0 MAF 0.01479	This study	Likely pathogenic
c.1217T>C	p.M406T	Wissinger et al. 2001 (16) SCV000700222	1 Disease-causing 2 Probably damaging 0.812 3 Damaging 0.03 4 HSF&MaxEnt: Potential alteration of splicing.	Complete Linker TM6-CNBD	No, single patient	No entry	Muraki-Oda et al. 2007: Functional assessment by heterologous *in vitro* expression (17)	Pathogenic
c.1279C>T	p.R427C	Wissinger et al. 2001 (16) SCV000700223	1 Disease-causing 2 Probably damaging 1.000 3 Damaging 0 4 HSF&MaxEnt: Potential alteration of splicing.	Complete Linker TM6-CNBD	Yes	107/276216/1 MAF 0.03874	Koeppen et al. 2008: Functional assessment by heterologous *in vitro* expression (21)	Pathogenic
c.1306C>T	p.R436W	Wissinger et al. 2001 (16) SCV000700224	1 Disease-causing 2 Probably damaging 1.000 3 Damaging 0 4 HSF&MaxEnt: Potential alteration of splicing.	Complete Linker TM6-CNBD	Yes	24/245446/0 MAF 9.778e-3	Muraki-Oda et al. 2007, Matveev et al. 2010: Functional assessment by heterologous *in vitro* expression (17, 22)	Pathogenic
c.1320G>A	p.W440*	Wissinger et al. 2001 (16) SCV000700225	1 Disease-causing, PTC 4 HSF&MaxEnt: Potential alteration of splicing.	-	Yes	1/245676/0 MAF 4.07e-3	-	Pathogenic
c.1777G>A	p.E593K	Wissinger et al. 2001 (16) SCV000700226	1 Disease-causing 2 Probably damaging 0.830 3 Tolerated 0.17 4 HSF&MaxEnt: Potential alteration of splicing.	High Loop αB-αC	No, single patient	3/245986/0 MAF 1.22e-2	Muraki-Oda et al. 2007, functional assessment by heterologous in vitro expression (17)	Pathogenic

Supplementary Information Material & Methods

Primers for PCR amplification and Sanger sequencing of CNGA3

PCR primers *CNGA3*

Exon	Primer forward 5‘-3‘	Primer reverse 5‘-3‘	PCR program
1	gcagcaggaactacaagag	agctgtggaaatgaccagag	94°C-4min, 40x 94°C-30sec, 55°C-30sec, 72°C-60sec, 72°C-5min, 8°C
2ab	cctgggatgaggatctgtg	gctggagtacggatgtca	94°C-4min, 35x 94°C-30sec, 58°C-20sec, 72°C-60sec, 72°C-5min, 8°C
3	cccttgagacagacagagag	ggctgtagagcatgtagtgc	94°C-4min, 35x 94°C-15sec, 55°C-15sec, 72°C-30sec, 72°C-5min, 8°C
4	cccgaggtaactaatcaca	gggagcaggagcactaa	94°C-4min, 35x 94°C-30sec, 55°C-30sec, 72°C-60sec, 72°C-5min, 8°C
5	catgtgactcccttgagact	gctgtccaggtgaagctc	94°C-4min, 35x 94°C-15sec, 55°C-15sec, 72°C-30sec, 72°C-5min, 8°C
6	attacatgatccagcgtctt	aaggtcatacagcttgttgg	94°C-4min, 35x 94°C-15sec, 55°C-15sec, 72°C-30sec, 72°C-5min, 8°C
7	tcagagtgcatttcctgtagt	gctttcaaagggtgagtaga	94°C-4min, 40x 94°C-30sec, 55°C-30sec, 72°C-90sec, 72°C-5min, 8°C

Sequencing primers *CNGA3*

Exon	Orientation	Sequencing primer 5‘-3‘
1	forward	gtagcccttgcccttga
2ab	forward	gtggctttccctgctaag
2ab-2	forward	ggggtggagttgagttgaagatt
3	forward	ggggtttgggggtgtgg
4	forward	cccgaggtaactaatcaca (same as PCR primer)
5	forward	ggctctctaaaaccctcca
6	reverse	tgtccaagggttccgtgtag
7-1	forward	gcatactgtgtagccgtgagg
7-2	forward	atgtttgaattctttgaccgca
7-3	forward	gtgggcaatgtgggctcc
7-4	forward	tggcagctacttcggggagat

PCR fragments were purified by treatment with ExoSAP-IT (GE Healthcare, Freiburg, Germany) and sequenced with BigDye Termination chemistry (Applied Biosystems, Darmstadt, Germany) with the above mentioned primers and following the protocol: 2 min 96°C - 25 cycles of 15 sec at 96°C, 15 sec at 55°C, 4 min at 60°C, hold at 8°C. The products were run on a capillary sequencer (ABI 3130, Applied Biosystems) and sequencing data were analyzed with the Sequencing Analysis software (version 5.2, Applied Biosystems) and sequence trace alignment software (SeqMan, DNASTAR, Madison, USA).

Primers for PCR amplification and Sanger sequencing of CNGB3.

The same primers were used for amplification and sequencing.

Exon	Primer forward 5'-3'	Primer reverse 5'-3'
1	cacccaagcagaagtatttt	tgaagataagcccgacac
2	ggaggctgaggttgattatt	cccatgttgctcattactg
3	tcccaggggaggtgttctt	gctaaaggggagagtggata
4	ttcccttatatctatttcttc	tgggagatccaaactaaac
5	catgcggtgtttggttaaga	acagggtttcttggtgatag
6	gcccggagcctcacagt	gtagcccaattagatgtta
7	tggctgagattggaaggaac	gcagaaacttcaggcttatc
8	ccagaaaggcatgtaaacac	tttgggaaaaattaagaatattg
9	ctctggaagtataataccatgc	catctgttctagaacatagtcc
10	cagtcaagacattgccatcag	agcatttaccagccattgaatgg
11	ttaagaagtttacattagcaca	tcaactcattaaaatagaagaa
12	agggcattagaaggaagtat	aacgaatgctttaaggatca
13	gaatctgatgcatctaattatg	gttggctgaagagagacctg
14	ggaatattggcctttagttg	tgacttatgtccgaaatcct
15	acccatgtctgtaaatactt	aaatctgagcgggaacttat
16	tgtgggacttagaggtga	aagcatatctcactgtgatcaag
17	caccattagagatggatggag	gcaggaagtattagtattag
18	gacagtctgtcttggtggt	gtcccagcatgtcgtttcc

All PCR amplifications were performed with the following program: denaturation at 94°C - 4min, 40 cycles of 94°C - 15sec, 50°C - 15sec, 72°C - 30sec, and a final extension at 72°C - 5min, cool to 8°C
PCR fragments were purified by treatment with ExoSAP-IT (GE Healthcare, Freiburg, Germany) and sequenced with BigDye Termination chemistry (Applied Biosystems, Darmstadt, Germany) with the following protocol: 2 min 96°C - 25 cycles with 15 sec at 96°C, 15 sec at 53°C, 4min at 60°C and hold at 8°C. The products were run on a capillary sequencer (ABI 3130, Applied Biosystems) and sequencing data were analyzed with the Sequencing Analysis software (version 5.2, Applied Biosystems) and sequence trace alignment software (SeqMan, DNASTAR, Madison, USA).

Primers for genotyping of mutant ES cells and mutant mice

Genotyping	Primer forward 5‘-3‘	Primer reverse 5‘-3‘	PCR program
Cnga3 **mice**	cttaggtttccttgaggcaagg	caagttccctatcctgaacacg + gcctgctctttactgaaggctc	94°C-3min, 30x 94°C-20sec, 58°C-20sec, 72°C-20sec, 72°C-5min, 8°C
Cngb3 **mice**	tgtggattcccagttattg	aatattgtagtctcttgcctt	94°C-3min, 30x 94°C-20sec, 58°C-20sec, 72°C-20sec, 72°C-5min, 8°C
Cngb3 **5‘ 1. targeting**	tccctttttatgtcttgggtggt	caagcttggctggacgtaaactc	94°C-4min, 34x 94°C-15sec, 63°C-30sec, 68°C-4min, 72°C-10min, 8°C
Exclusion of ***Rd8*** **mutation**	gcccctgtttgcatggaggaaacttggaagacagctacagttcatat	gccccatttgcacactgatgac	94°C-2min, 35x 94°C-15sec, 62°C-30sec, 72°C-30sec, 72°C-4min, 8°C. Restriction digestion with NdeI

Primers for PCR amplification of Southern blot probes

Probe	Primer forward 5'-3'	Primer reverse 5'-3'
5‘	gtatattgtttcatgagattcttg	aatcacgtgcccagacag
3’	cttcatagctactagaatgaatg	atatggtccatgcaggcttg

PCR amplification weas performed with the following program: denaturation at 94°C – 4 min, 34 cycles of 95°C – 15 sec, 63°C – 30 sec, 68°C – 2 min, and a final extension at 72°C – 10 min, cool to 8°C.

Primers for PCR amplification of the Cngb3 antigen for the anti-CNGB3 rabbit antiserum

	Primer forward 5'-3'	Primer reverse 5'-3'
Cngb3	ggatccgatgttaaaatcact	aagcttcccgatctgtgtag

cDNA synthesis was performed at 50°C for 30 min. PCR amplification was performed with the following program: denaturation at 94°C – 2 min, 40 cycles of 94°C – 15 sec, 55°C – 30 sec, 68°C – 1 min, and a final extension at 72°C – 5 min, cool to 8°C.

Supplementary References

1. Renner, A.B., Tillack, H., Kraus, H., Kohl, S., Wissinger, B., Mohr, N., Weber, B.H., Kellner, U., and Foerster, M.H. 2004. Morphology and functional characteristics in adult vitelliform macular dystrophy. *Retina* 24:929-939.
2. Ding, X.Q., Harry, C.S., Umino, Y., Matveev, A.V., Fliesler, S.J., and Barlow, R.B. 2009. Impaired cone function and cone degeneration resulting from CNGB3 deficiency: down-regulation of CNGA3 biosynthesis as a potential mechanism. *Hum Mol Genet* 18:4770-4780.
3. Schwarz, J.M., Cooper, D.N., Schuelke, M., and Seelow, D. 2014. MutationTaster2: mutation prediction for the deep-sequencing age. *Nat Methods* 11:361-362.
4. Adzhubei, I.A., Schmidt, S., Peshkin, L., Ramensky, V.E., Gerasimova, A., Bork, P., Kondrashov, A.S., and Sunyaev, S.R. 2010. A method and server for predicting damaging missense mutations. *Nat Methods* 7:248-249.
5. Kumar, P., Henikoff, S., and Ng, P.C. 2009. Predicting the effects of coding non-synonymous variants on protein function using the SIFT algorithm. *Nat Protoc* 4:1073-1081.
6. Desmet, F.O., Hamroun, D., Lalande, M., Collod-Beroud, G., Claustres, M., and Beroud, C. 2009. Human Splicing Finder: an online bioinformatics tool to predict splicing signals. *Nucleic Acids Res* 37:e67.
7. Richards, S., Aziz, N., Bale, S., Bick, D., Das, S., Gastier-Foster, J., Grody, W.W., Hegde, M., Lyon, E., Spector, E., et al. 2015. Standards and guidelines for the interpretation of sequence variants: a joint consensus recommendation of the American College of Medical Genetics and Genomics and the Association for Molecular Pathology. *Genet Med* 17:405-424.
8. Landrum, M.J., Lee, J.M., Riley, G.R., Jang, W., Rubinstein, W.S., Church, D.M., and Maglott, D.R. 2014. ClinVar: public archive of relationships among sequence variation and human phenotype. *Nucleic Acids Res* 42:D980-985.
9. Kohl, S., Varsanyi, B., Antunes, G.A., Baumann, B., Hoyng, C.B., Jagle, H., Rosenberg, T., Kellner, U., Lorenz, B., Salati, R., et al. 2005. CNGB3 mutations account for 50% of all cases with autosomal recessive achromatopsia. *Eur J Hum Genet* 13:302-308.
10. Kohl, S., Baumann, B., Broghammer, M., Jagle, H., Sieving, P., Kellner, U., Spegal, R., Anastasi, M., Zrenner, E., Sharpe, L.T., et al. 2000. Mutations in the CNGB3 gene encoding the beta-subunit of the cone photoreceptor cGMP-gated channel are responsible for achromatopsia (ACHM3) linked to chromosome 8q21. *Hum Mol Genet* 9:2107-2116.
11. Peng, C., Rich, E.D., and Varnum, M.D. 2003. Achromatopsia-associated mutation in the human cone photoreceptor cyclic nucleotide-gated channel CNGB3 subunit alters the ligand sensitivity and pore properties of heteromeric channels. *J Biol Chem* 278:34533-34540.
12. Michaelides, M., Aligianis, I.A., Ainsworth, J.R., Good, P., Mollon, J.D., Maher, E.R., Moore, A.T., and Hunt, D.M. 2004. Progressive cone dystrophy associated with mutation in CNGB3. *Invest Ophthalmol Vis Sci* 45:1975-1982.
13. Bright, S.R., Brown, T.E., and Varnum, M.D. 2005. Disease-associated mutations in CNGB3 produce gain of function alterations in cone cyclic nucleotide-gated channels. *Mol Vis* 11:1141-1150.
14. Nishiguchi, K.M., Sandberg, M.A., Gorji, N., Berson, E.L., and Dryja, T.P. 2005. Cone cGMP-gated channel mutations and clinical findings in patients with achromatopsia, macular degeneration, and other hereditary cone diseases. *Hum Mutat* 25:248-258.
15. Meighan, P.C., Peng, C., and Varnum, M.D. 2015. Inherited macular degeneration-associated mutations in CNGB3 increase the ligand sensitivity and spontaneous open probability of cone cyclic nucleotide-gated channels. *Front Physiol* 6:177.
16. Wissinger, B., Gamer, D., Jagle, H., Giorda, R., Marx, T., Mayer, S., Tippmann, S., Broghammer, M., Jurklies, B., Rosenberg, T., et al. 2001. CNGA3 mutations in hereditary cone photoreceptor disorders. *Am J Hum Genet* 69:722-737.
17. Muraki-Oda, S., Toyoda, F., Okada, A., Tanabe, S., Yamade, S., Ueyama, H., Matsuura, H., and Ohji, M. 2007. Functional analysis of rod monochromacy-associated missense mutations in the CNGA3 subunit of the cone photoreceptor cGMP-gated channel. *Biochem Biophys Res Commun* 362:88-93.
18. Reuter, P., Koeppen, K., Ladewig, T., Kohl, S., Baumann, B., Wissinger, B., and Achromatopsia Clinical Study, G. 2008. Mutations in CNGA3 impair trafficking or function of cone cyclic nucleotide-gated channels, resulting in achromatopsia. *Hum Mutat* 29:1228-1236.
19. Thiadens, A.A., Roosing, S., Collin, R.W., van Moll-Ramirez, N., van Lith-Verhoeven, J.J., van Schooneveld, M.J., den Hollander, A.I., van den Born, L.I., Hoyng, C.B., Cremers, F.P., et al. 2010. Comprehensive analysis of the achromatopsia genes CNGA3 and CNGB3 in progressive cone dystrophy. *Ophthalmology* 117:825-830 e821.

20. Liu, C., and Varnum, M.D. 2005. Functional consequences of progressive cone dystrophy-associated mutations in the human cone photoreceptor cyclic nucleotide-gated channel CNGA3 subunit. *Am J Physiol Cell Physiol* 289:C187-198.
21. Koeppen, K., Reuter, P., Kohl, S., Baumann, B., Ladewig, T., and Wissinger, B. 2008. Functional analysis of human CNGA3 mutations associated with colour blindness suggests impaired surface expression of channel mutants A3(R427C) and A3(R563C). *Eur J Neurosci* 27:2391-2401.
22. Goto-Omoto, S., Hayashi, T., Gekka, T., Kubo, A., Takeuchi, T., and Kitahara, K. 2006. Compound heterozygous CNGA3 mutations (R436W, L633P) in a Japanese patient with congenital achromatopsia. *Vis Neurosci* 23:395-402.